Experimental Hematology

Experimental Hematology 2019;79:35–46

REGULAR SUBMISSION

Depletion of the transcriptional coactivators CREB-binding protein or EP300 downregulates CD20 in diffuse large B-cell lymphoma cells and impairs the cytotoxic effects of anti-CD20 antibodies

Annarita Scialdone[a,1], Somayeh Khazaei[a,1], Muhammad Sharif Hasni[b], Andreas Lennartsson[c], Urban Gullberg[a], and Kristina Drott[a,d]

[a]*Department of Hematology and Transfusion Medicine, Lund University, Lund, Sweden;* [b]*Institute of Biochemistry, University of Balochistan, Quetta, Pakistan;* [c]*Department of Biosciences and Nutrition, Karolinska Institutet, Huddinge, Sweden;* [d]*Clinic of Oncology, Skåne University Hospital, Lund, Sweden*

(Received 14 June 2019; revised 11 October 2019; accepted 17 October 2019)

Monoclonal antibodies targeting CD20 are central in the treatment of B-cell lymphomas. In diffuse large B-cell lymphoma (DLBCL), inactivating mutations of the histone acetyltransferases CREB-binding protein (CBP) and EP300 are common. Moreover, knockdown of CBP in DLBCL has been shown to result in aberrant transcriptional silencing. Expression of CD20 is sensitive to epigenetic manipulation, and histone deacetylase inhibitors have been found to potentiate treatment with anti-CD20 antibodies. Therefore, we studied the role of CBP and EP300 depletion on CD20 expression and effects of the anti-CD20 antibodies rituximab and obinutuzumab in DLBCL cells. Levels of CBP and EP300 were reduced by shRNA in the germinal centre-derived diffuse large B-cell lymphoma cell line SU-DHL4. The levels of CD20 mRNA and protein were determined by quantitative polymerase chain reaction, Western blot, and flow cytometry. Binding of the transcription factors PU.1 and FOXO1 to the CD20 promoter was determined by chromatin immunoprecipitation coupled with quantitative polymerase chain reaction. Response to the monoclonal anti-CD20 antibodies rituximab and obinutuzumab in CBP- or EP300-depleted cells was assessed by complement-dependent cell death, direct cell death, and antibody-dependent cellular cytotoxicity (ADCC). Our results suggest that depletion of CBP and EP300 levels leads to a strong reduction of CD20 expression, accompanied by reduced binding of PU.1 to the CD20 promoter. In CBP-depleted, but not EP300-depleted cells, increased binding of FOXO1 to the CD20 promoter was observed. Interestingly, CBP or EP300 depletion leads to decreased complement-dependent cell death and direct cell death in response to rituximab and obinutuzumab, which was most pronounced in response to rituximab in CBP-depleted cells. Our data suggest that inactivating mutations of CBP, and to a lesser extent EP300, may impair the response to anti-CD20 antibodies. However, these observations should be analyzed in future clinical trials.

Diffuse large B-cell lymphoma (DLBCL) is the most common aggressive B-cell lymphoma.

Standard first-line treatment of DLBCL is chemotherapy consisting of a combination of cyclophosphamide, doxorubicin, vincristine, and prednisone (CHOP). It has been more than 10 years since addition of the anti-CD20 antibody rituximab became the international

Offprint requests to: Kristina Drott, Clinic of Oncology, Skåne University Hospital, Lund, Sweden;
E-mails: kristina.drott@med.lu.se; kristina.drott@gmail.com

[1]AS and SK have contributed equally to this article.

Supplementary material associated with this article can be found in the online version at doi:10.1016/j.exphem.2019.10.004.

https://doi.org/10.1016/j.exphem.2019.10.004

clinical standard (R-CHOP), leading to improved progression-free, event-free, disease-free, and overall survival. Although R-CHOP leads to remission in 85% of patients, about 40% of these relapse, often with disease that is resistant to rituximab [1].

A suggested mechanism for resistance to anti-CD20 antibodies is transcriptional downregulation of CD20 mRNA and the number of CD20 molecules on the cell surface [2]. Hence, rituximab-treated DLBCL patients often relapse with CD20-negative disease [3]. That CD20 expression is regulated by epigenetic mechanisms in DLBCL is supported by an increasing amount of data. Several authors describe epigenetic silencing of CD20 expression via histone deacetylases (HDACs) as a mechanism conferring resistance to rituximab in B-cell lymphomas [4,5]. Moreover, Shimizu et al. [6] reported that epigenetic modulation through inhibition of HDACs can increase acetylation of the CD20 promoter, resulting in recruitment of the Sp1 transcription factor and increased expression of CD20 mRNA and protein in B-cell lymphoma cell lines. This is confirmed *in vivo* by our own data on valproate-mediated inhibition of histone deacetylation in three DLBCL patients, resulting in increased CD20 expression in these patients [7].

Interestingly, DLBCL is characterized by heterozygous mutations in enzymes regulating posttranslational histone modifications. For example, the histone methyl transferases KMTD2 and EZH2 are mutated in 30% and 10% of DLBCL cases, respectively. Moreover, the histone acetyltransferase CREB-binding protein (CBP) and its paralogue E1A-associated protein p300 (EP300) have inactivating mutations of their acetyltransferase domain in 30% and 10% of cases, respectively—mutations that are often mutually exclusive [8–10]. Moreover, loss of CBP facilitates the development of germinal center (GC)-derived lymphomas in mice. Interestingly, this has been suggested to depend on a dysregulated epigenetic landscape in these cells, as loss of CBP results in unopposed deacetylation at enhancers of B-cell signaling and immune response genes [11]. CBP and EP300 activate transcription by histone acetylation or by regulation of transcription factor activity through direct interaction or by acetylation [12]. Therefore, we hypothesized that CBP and EP300 could counteract the activity of HDACs in CD20 regulation, and that inactivating mutation of CBP or EP300 could have a negative impact on CD20 expression and hence on the response to anti-CD20 antibodies in DLBCL.

To create a model for the response to anti-CD20 antibodies in a CBP or EP300 heterozygous background, levels of CBP and EP300 were knocked down by RNA interference in the germinal centre-derived DLBCL cell line SU-DHL4. Our data suggest that depletion of CBP or EP300 strongly affects CD20 expression and the response to the anti-CD20 antibodies rituximab and obinutuzumab.

Methods

Cell culture and DNA sequencing

The SU-DHL4 and WSU-NHL diffuse large B-cell lymphoma cell lines were purchased from Leibniz-Institute DSMZ-German Collection of Microorganisms and Cell Cultures (Braunschweig, Germany) and were cultured for no more than 20 passages. Cells were maintained at 0.5×10^6 cells/mL in RPMI-1640 medium supplemented with 10% fetal bovine serum (both from Invitrogen; RPMI/10% FBS) at 37°C with 5% CO_2. Exons 24 to 31 of CBP and EP300, encoding the acetyltransferase domains of both proteins, were amplified from genomic DNA and sequenced. Primer sequences are provided in Supplementary Tables E1 and E2 (online only, available at www.exphem.org).

Knockdown of CBP and EP300 in SU-HDL4 cells

Scrambled shRNA lentiviral vector and CBP or EP300-targeting shRNA were purchased from Sigma-Aldrich (No. SHC002, St. Louis, MO). Lentiviral particles were produced at the core facility Vector Unit, Lund University. Lentiviral packaging of TRC2-pLKO shRNA vectors was done in HEK293T cells. Briefly, HEK293T were plated 1 day in advance to reach a confluence of 50%–70% at the time of transfection. Expression vectors pCMV Δ8.91 (14 μg), VSV-G pMDG plasmid (6 μg), and the TRC2-pLKO (20 μg) lentiviral vector were co-transfected using 0.5 mol/L $CaCl_2$ sterile filtered solution. After overnight incubation at 37°C in 5% CO_2, the medium was discarded and fresh Dulbecco's modified Eagle's medium (DMEM)–10% FBS was added to the plates. Viral supernatants were collected twice during the following 48 hours and filtered with a 0.45-μm PES low-clogging, low-protein-binding filter. The lentiviral particles were directly used to transduce target cells or stored at −80°C. For transduction of cells, non-tissue culture-coated well plates were coated with RetroNectin (Takara Clontech, Otsu, Shiga, Japan) for 2 hours at room temperature, and blocked with 2% bovine serum albumin for 30 min at room temperature. After this, virus-containing medium produced as described above was added, and the lentiviral particles were allowed to bind for 1 hour at 4°C under centrifugation, after which 2×10^6 cells were added and cultured in the virus-coated wells for 48 hours at 37°C with 5% CO_2. Transduced cells were selected for a further 72 hours of culture in the presence of 0.7 μg/mL puromycin (Gibco, Gaithersburg, MD).

Reverse transcription and qPCR

Total RNA was isolated using the RNeasy Mini Kit (Qiagen, Hilden, Germany) according to the manufacturer's recommendation. Synthesis of cDNA was carried out using a high-capacity reverse transcription kit (Applied Biosystems, Waltham, MA) according to the protocol provided by the manufacturer. qPCR was carried out using TaqMan probe-based chemistry (Applied Biosystems) with the probes for CBP (Hs00231733-m1), EP300 (Hs00914223-m1), CD20 (Hs00544819-m1 MS4A1), PU.1 (Hs02786711-m1), FOXO1 (Hs231106-m1), and GAPDH (Hs02758991-g1). The

amplification reactions were all performed in duplicate, in a StepOnePlus machine (Applied Biosystems). Data were collected and analyzed using Applied Biosystems' StepOne Real-Time PCR Software, Version 2.0. The relative expression of the probed genes was calculated with the $\Delta\Delta Ct$ method [13], using GAPDH as equal loading control.

SDS-PAGE and Western blot

Cells were lysed in lysis buffer (50 mmol/L Tris–HCl, pH 7.8, 150 mmol/L NaCl, 1 mmol/L ethylenediamine tetraacetic acid (EDTA, 1% Nonidet P-40) followed by sonication (4 cycles) using a Bioruptor PICO (Diagenode, Seraing, Belgium). Loading samples were prepared with Laemmli buffer (Bio-Rad, Hercules, CA) with β-mercaptoethanol (Scharlau Chemicals, Barcelona, Spain) and protease inhibitor (Roche, Basel, Switzerland). Proteins were separated by sodium dodecyl sulfate–polyacrylamide gel electrophoresis (SDS–PAGE; 4%–20% Mini-Protean TGX gel, Bio-Rad) and transferred to a nitrocellulose membrane (Trans-Blot Turbo Midi Nitrocellulose Transfer Packs, Bio-Rad). The primary antibodies used were polyclonal rabbit anti-CBP (sc369, Santa Cruz Biotechnology, Dallas, TX), monoclonal mouse anti-EP300 (sc48343, Santa Cruz Biotechnology), polyclonal mouse anti-CD20 (ab88247, Abcam, Cambridge, UK), rabbit anti-PU.1 (2266s, Cell Signaling, Leiden, Netherlands), monoclonal rabbit FOXO1 (2880s, Cell Signaling, Danvers, MA), and monoclonal mouse anti-γ-tubulin (T5326, Sigma-Aldrich). The EZ-ECL kit (Biological Industries, Kibbutz Beit Haemek, Israel) was used to detect protein bands with a ChemiDoc XRS+ system (Bio-Rad). Band intensity was analyzed using Bio-Rad's Image Lab software and normalized to γ-tubulin.

Flow cytometry

To evaluate surface CD20 expression, 5×10^5 cells were centrifuged, washed, and incubated with the mouse monoclonal anti-human CD20 (L27) PE (Catalog No. 347201, BD Pharmingen) in cold 2% FBS/phosphate-buffered saline (PBS) (Gibco). After 20 min at room temperature, samples were washed and resuspended in 2% FBS–PBS to be analyzed. The amount of membrane CD20 molecules was assessed by flow cytometry using the FACS Canto BD (BD Biosciences). Unlabeled cells were used to exclude the background in each experiment.

Chromatin immunoprecipitation

ChIP experiments were performed using the EZ-ChIP kit (Catalog No. 17-371, Merck Millipore, Darmstadt, Germany), according to the manufacturer's instructions. Chromatin was cross-linked with 1% formaldehyde (Sigma-Aldrich) for 10 min at room temperature. The reaction was stopped with glycine 1 × (Millipore), followed by two washes in cold PBS (Gibco). Cells were lysed in SDS lysis buffer provided by the manufacturer (100 μL × 10^6 cells) and subjected to sonication (6 cycles, 1 min each: 30 sec on–30 sec off) using a Bioruptor PICO (Diagenode, Seraing, Belgium). The rabbit anti-PU.1 (2266s, Cell Signaling, Danvers, MA) and monoclonal rabbit FOXO1 (2880s, Cell Signaling, Danvers, MA) antibodies were added to protein G–agarose precleared chromatin lysate and incubated overnight at 4°C. Immunoprecipitation was done using protein G-agarose pull-down followed by reverse of cross-linking. ChIP samples were analyzed by SYBR Green qRT-PCR using 4 μL of immunoprecipitated chromatin and input as control (1% of the immunoprecipitated material). Specific primers were used to amplify the CD20 promoter in the region between −273 and −88 bp, which includes both the FOXO-binding region (−182 and −88bp) and the PU.1 binding site (−161 and −148 bp): 5′- TAACGGCCCATCTTTGACCA -3′ (forward) and 5′- TGGGCTTCGCTCCAATTACT -3′ (reverse). The binding of each transcriptional factor to the CD20 promoter was calculated as a percentage of input. Values from cells transduced with specific shRNA were normalized to values from cells transfected with scrambled shRNA, and the fold change is illustrated in the graphs.

Complement-dependent cytotoxicity

Cells were seeded at a concentration of 1×10^6/mL in RPMI/10% FBS supplemented with 10% whole human serum in round bottom 96-well plates to a final volume of 100 μL/well. Rituximab (A2009, Selleckchem, Houston, TX, USA) or obinutuzumab (Roche) was added at a final concentration of either 1 or 10 μg/mL. Cells with only whole human serum were used as control. After 2 hours of incubation at 37°C and 5% CO_2, viability was determined by staining with propidium iodide (PI) (BD Pharmingen, San Diego, CA). PI at a final concentration of 4 μg/mL was added to the 96 well-round bottom plates, and the percentages of PI-positive cells were measured by flow cytometry (BD LSRFortessa, San Jose, CA).

Direct cell death

Cells were incubated in RPMI supplemented with 10% heat-inactivated fetal calf serum and 10% heat-inactivated whole human serum with or without rituximab or obinutuzumab, at a concentration of either 1 or 10 μg/mL for 2 hours at 37°C and 5% CO_2. A fluorescein isothiocyanate (FITC) Annexin V apoptosis detection kit (BD Pharmingen, San Diego, CA) and PI were utilized to stain the dead cells.

Antibody-dependent cellular cytotoxicity

Antibody-dependent cellular cytotoxicity (ADCC) in SU-DHL4 cells was analyzed using the LIVE/DEAD Cell-Mediated Cytotoxicity Kit according to the instructions of the manufacturer (Invitrogen).

Double staining with the green fluorescent membrane dye lipophilic carbocyanine (DIOC18) and PI was used to discriminate between dead target cells ($DIOC18^+PI^+$) and dead effector cells ($DIOC18^-PI^+$). To this aim, target SU-DHL4 cells were pre-labeled with DIOC18 at 37°C and 5% CO_2 for 20 min, then washed and incubated with the effectors. Natural killer (NK) cells, isolated from whole human blood using the MACSxpress Whole Blood NK Cell Isolation Kit (Miltenyi Biotec, Bergisch Gladbach, Germany), were used as effector cells. Target and effector cells were added to round-bottom 96-well plates; each well contained 5×10^4 target cells and 1×10^5 effector cells at an E:T ratio of 2:1 in a final volume of 150 μL. The anti-CD20 monoclonal antibody

rituximab or obinutuzumab was added to the plate to final concentrations of either 1 or 10 μg/mL and incubated for 2 hours at 37°C and 5% CO_2. Wells containing only target and effector cells without any antibody were utilized as a control. After incubation, PI (4 μg/mL) was added to each well, and $DIOC18^+PI^+$ cells were analyzed by flow cytometry utilizing a BD LSRFortessa.

Statistical analysis

Statistical analysis was performed using the unpaired Student two-tailed *t* -test and two-way analysis of variance (ANOVA) test. Asterisks represent conventional significance levels: $*p \leq 0.,05$, $**p < 0.01$, $***p < 0.001$. The SEM was calculated when there were three or more samples. In experiments with rituximab or obinutuzumab, the SEM was calculated from three independent experiments, where each antibody concentration was tested in technical duplicates within each experiment.

Results

Expression of wild-type CBP and EP300 in SUDHL4 cells

Monoallelic inactivating mutations of CBP or EP300 in DLBCL suggest that reduced functional levels of the enzymes are important for lymphomagenesis [9]. To study the effects of reduced levels of functional protein, the GC-derived diffuse large B-cell lymphoma cell line SUDHL4 was selected, based on previous reports indicating that this cell line expresses wild-type (WT) CBP and EP300 genes [9]. CBP WT and EP300 WT were verified by sequencing of exons 24 to 31 of CBP and EP300, encoding the commonly mutated acetyltransferase domain [9] (data not shown).

Downregulation of CBP and EP300 in SU-DHL4 cells leads to reduction of CD20 expression

To reduce the functional levels of CBP or EP300, SU-DHL4 cells were transiently transduced with shRNA directed against CBP or EP300, as described under Methods. Cells transduced with a non-targeting−scrambled shRNA (shCTRL) were used as control. After puromycin selection, mRNA and protein levels of CBP and EP300 were assessed by qPCR and Western blot, respectively, revealing the expected reduction of CBP and EP300 mRNA (Figure 1A, B) and protein (Figure 1D, E) levels in response to shRNA transduction. No effects on the viability of the CBP- or EP300-depleted cells was detected as judged by trypan blue exclusion (Supplementary Figure E1, online only, available at www.exphem.org).

CD20 expression has been reported to be sensitive to manipulation of histone acetylation [6,7]. Moreover, Zhang et al. [14] found that the CD20 isoform MS4A4C is downregulated in the B cells of CBP haploinsuffiencient mice. Therefore, we investigated CD20 expression in the shRNA transduced cells. Interestingly, CBP or EP300 knockdown resulted in significant repression of CD20 mRNA and protein in SU-DHL4 cells (Figure 1C, F). Moreover, as judged by flow cytometry, CD20 cell surface expression was significantly reduced in both shCBP and shEP300 transduced cells, as compared with the control (Figure 1G). This reduction was more pronounced in CBP-depleted than in EP300-depleted cells. Downregulation of CD20 mRNA in response to depletion of CBP or EP300 was confirmed in the GC B-cell lymphoma cell line WSU-NHL (Supplementary Figure E2, online only, available at www.exphem.org). AS WSU-NHL cells carry an inactivating mutation in the histone acetyltransferase domain of CBP [15], experiments were hereafter conducted in SU-DHL4 cells, pertaining to wild-type phenotypes of CBP and EP300 genes. Taken together, these data suggest that knockdown of either CBP or EP300 downregulates CD20 expression.

Expression of PU.1 is reduced after knockdown of CBP

The results described above indicate that the histone acetyltransferases CBP and EP300 have a positive influence on CD20 expression. This notion is consistent with previous reports that histone deacetylase inhibitors acetylate the CD20 promoter and upregulate levels of CD20 [6,7]. Therefore, the acetylation status of H3K9 and H3K27 in the CD20 promoter of CBP or EP300 knockdown SU-DHL4 cells was assessed. However, no obvious effects of CBP or EP300 knockdown on H3K9 or H3K27 acetylation were observed (data not shown). Besides histone acetylation, CBP and EP300 also have a potential role in transcriptional regulation by direct acetylation of certain transcription factors [16], including PU.1 and FOXO1.

PU.1 is a transcriptional factor that is crucial for B-cell and macrophage development [17]. PU.1 binds the CD20 promoter [4] and induces expression of CD20 [18–20]. CBP- and EP300-mediated acetylation of PU.1 has been suggested to affect its DNA-binding capacity and interaction with other transcription factors [21].

FOXO1 has critical roles in early B-cell differentiation [22]. FOXO1 acts as a transcriptional repressor of CD20 through binding to the CD20 promoter [23]. CBP and EP300 acetylate FOXO1, resulting in a reduction of the DNA binding of FOXO1 [24–26].

Given the role of PU.1 and FOXO1 in the regulation of CD20 and its functional interactions with CBP and EP300, we hypothesized that modulation of these transcription factors could contribute to the decrease in CD20 expression in response to knockdown of CBP or EP300. First, we determined PU.1 and FOXO1

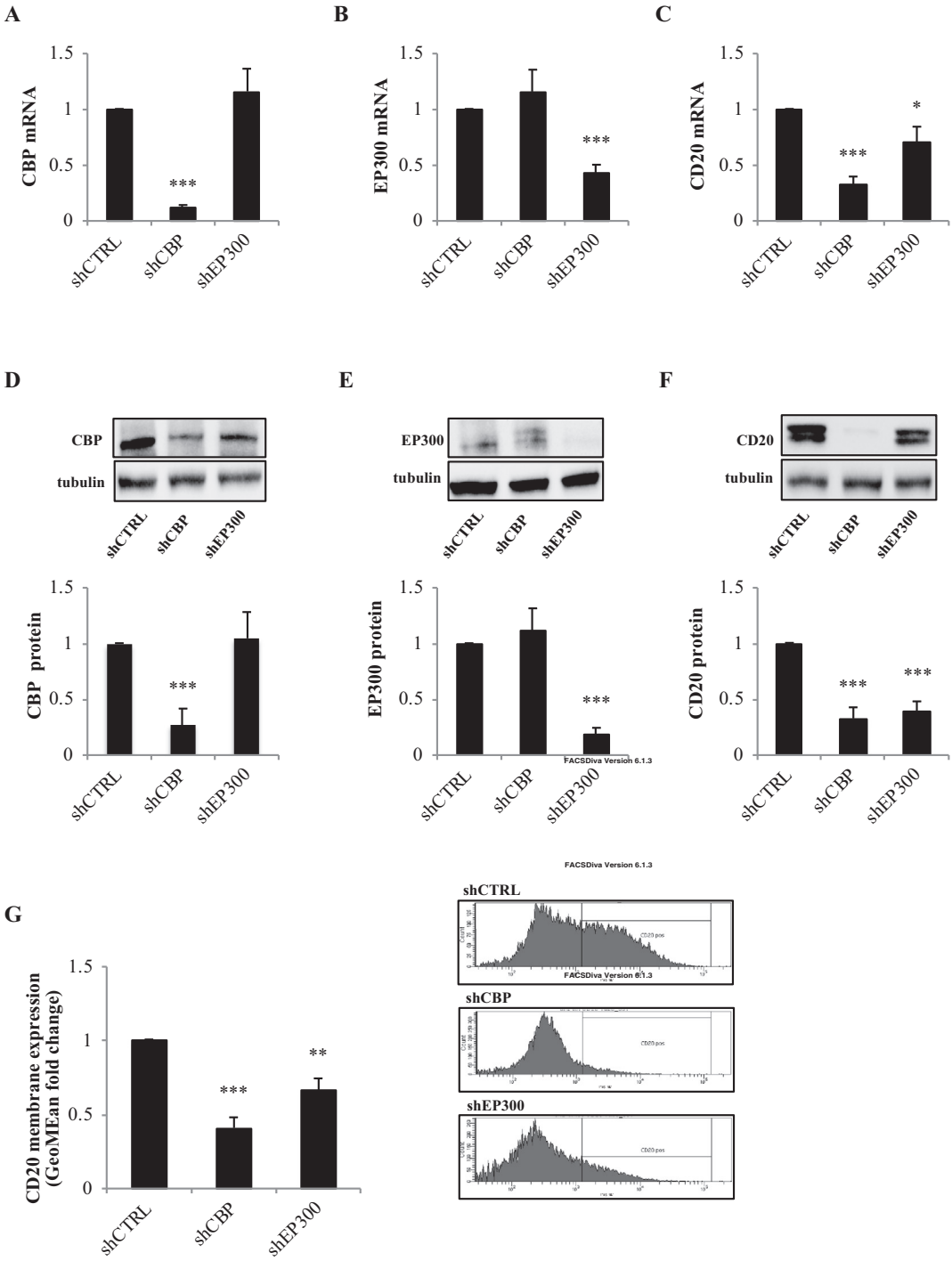

Figure 1. Downregulation of CBP or EP300 leads to decreased expression of CD20 in SU-DHL4 cells. SU-DHL4 cells were transduced with shRNA targeting either CBP or EP300. Expression of CBP **(A)**, EP300 **(B),** and CD20 **(C)** mRNA was determined by qPCR (±SEM, $n = 9$). CBP **(D)**, EP300 **(E),** and CD20 **(F)** protein was assessed by Western blot. shCTRL was utilized as a negative control and γ-tubulin as an equal loading control. Band intensity was estimated by densitometric analysis with Image Lab software. Results are presented as a fold change in band intensities versus control (±SEM, $n = 5$). Analysis of CD20 expression on the cell surface in CBP or EP300 knockdown cells was assessed by flow cytometry using a phycoerythrin-conjugated anti-CD20 antibody **(G)**. The bar plot represents the GeoMean fold change of CD20 expression in control and CBP or EP300 knockdown SU-DHL4 cells (±SEM, $n > 5$). An example of flow cytometry histograms showing the CD20-positive and CD20-negative fractions of shCTR, shCBP, and shEP300 transduced SU-DHL4 cells is shown. Statistical significance was determined with two-tailed unpaired Student t tests. Asterisks indicate statistical significance ($*p \leq 0.05$, $**p \leq 0.01$, $***p \leq 0.001$). Nonsignificant p values are not shown in the graph.

expression in both shCBP and shEP300 transduced cells by qPCR and Western blot. PU.1 mRNA (Figure 2A) and protein (Figure 2C) levels were significantly reduced in shCBP transduced SUDHL4 as compared with the control, whereas PU.1 expression was not decreased in EP300 knockdown cells (Figure 2A, C). FOXO1 expression was not changed after the knockdown of either CBP or EP300 (Figure 2B, D). These results indicate that CBP can affect the levels of PU.1, which potentially has consequences for the regulation of CD20. However, in EP300 knockdown cells, a reduction in PU.1 could not be detected despite the reduced expression of CD20.

PU.1 and FOXO1 binding to the CD20 promoter

To investigate whether knockdown of CBP or EP300 affects binding of PU.1 or FOXO1 to the CD20 promoter, we performed ChIP-qPCR analyses in CBP and EP300 knockdown cells. As illustrated in Figure 3B, PU.1 binding to the CD20 promoter was significantly reduced after knockdown of either CBP or EP300. This is consistent with the above-described results indicating reduced expression of CD20 in response to both shCBP and shEP300, and with a role for PU.1 in CD20 regulation in a CBP- and EP300-depleted context. However, knockdown of CBP resulted in a smaller total amount of PU.1 (Figure 2A, C), as well as reduced PU.1

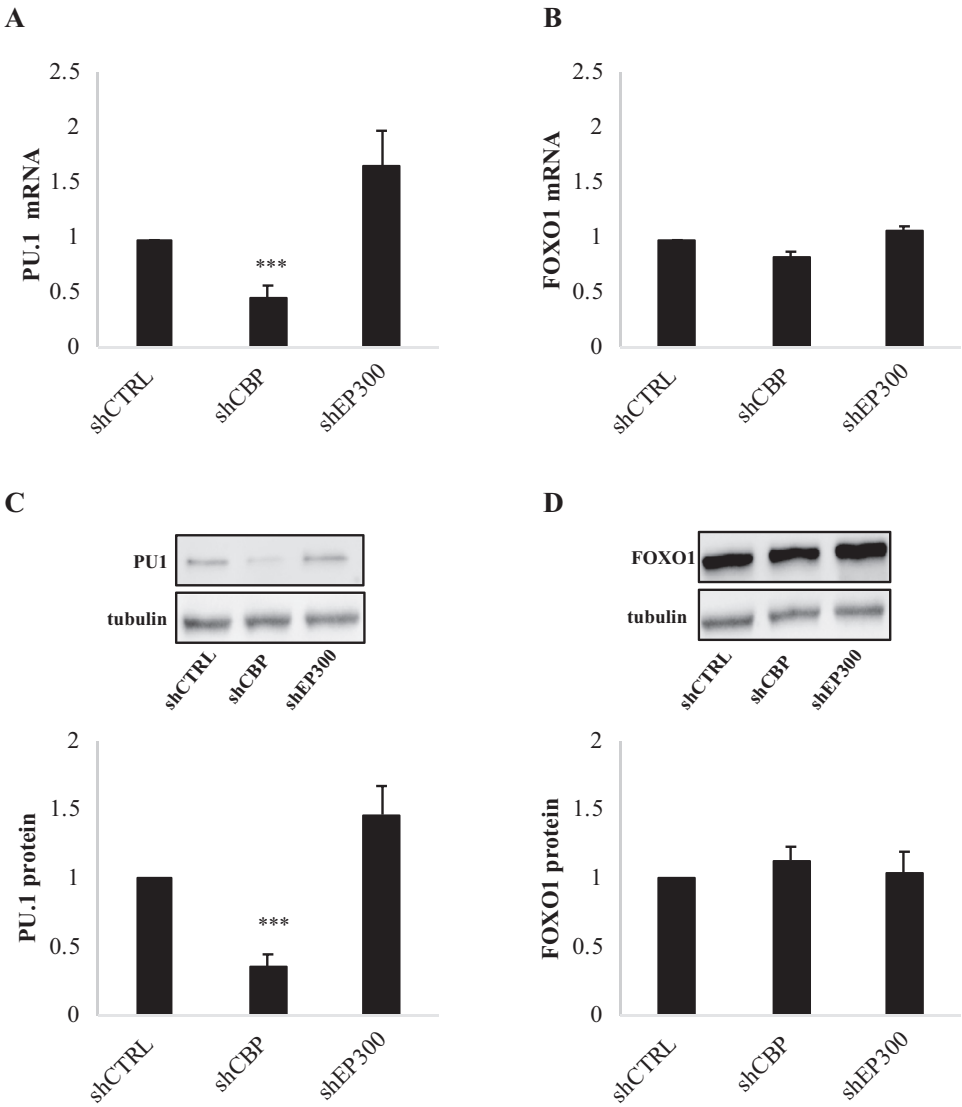

Figure 2. **(A, B)** Levels of PU.1 and FOXO1 in knockdown CBP or EP300 cells. Levels of PU.1 and FOXO1 mRNA were assessed by qPCR in CBP or EP300 knockdown cells. **(C, D)** Protein levels of PU.1 and FOXO1 were assessed by Western blot. The fold change in band intensities as measured by densitometry versus controls is shown (±SEM). Statistical significance was determined with two-tailed unpaired Student *t* tests. Asterisks indicate statistical significance (***$p \leq 0.001$, $n = 5$). Nonsignificant *p* values are not shown in the graph.

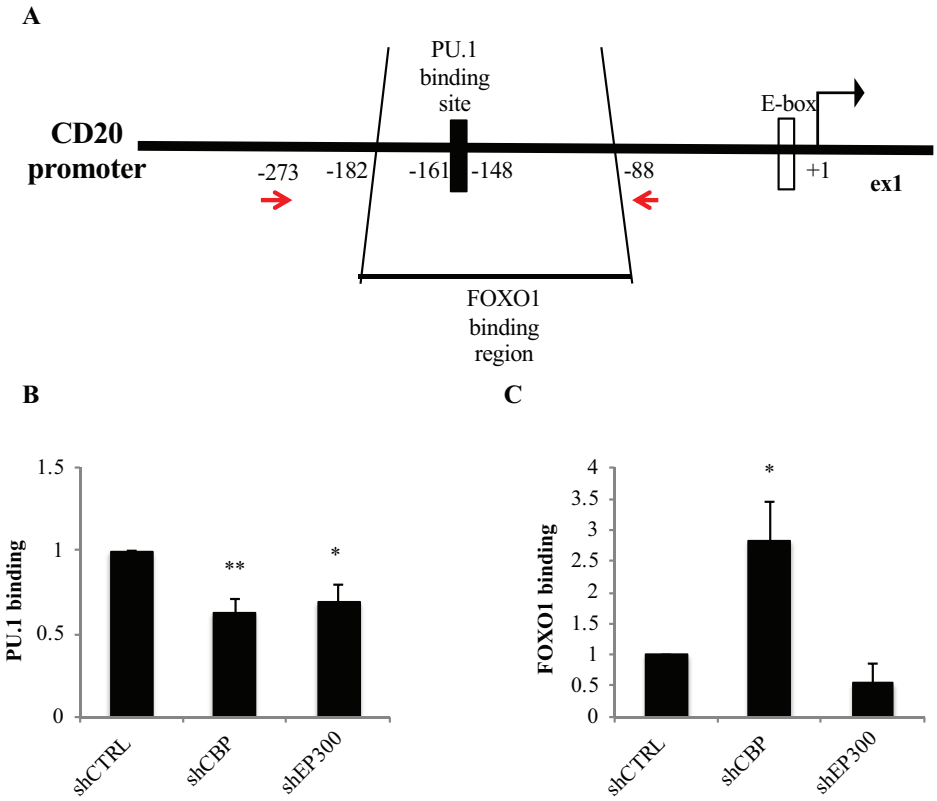

Figure 3. Knockdown of CBP or EP300 affects binding of PU.1 and FOXO1 to the CD20 promoter. Schematic presentation of the CD20 promoter revealing the FOXO1 binding region and PU.1 binding site **(A)** [6,23]. Primers used to amplify the region between −273 and −88 bp are represented by *red arrows*. Binding of PU.1 and FOXO1 to the CD20 promoter in CBP or EP300 knockdown SU-DHL4 cells was analyzed by ChIP-qPCR. qPCR was performed using primers specific for the region including the PU.1 **(B)** and FOXO1 **(C)** binding sites within the CD20 promoter, as specified under Methods and above. Results are presented as fold change in the transcription factor promoter occupancy in shCBP or shEP300 samples versus shCTRL (±SEM). Statistical significance was determined with two-tailed unpaired Student *t* tests. Asterisks indicate statistical significance ($*p \leq 0.05$, $**p \leq 0.01$, $n = 4$). Nonsignificant *p* values are not shown in the graph.

binding to the promoter, while EP300 knockdown affected PU.1 promoter binding (Figure 3B) without affecting total PU.1 levels (Figure 2A, C). This suggests posttranslational regulation of PU.1 in response to EP300 knockdown. In addition, based on these data, posttranslational regulation of PU.1 cannot be excluded in response to CBP knockdown.

Interestingly, the binding of the CD20 repressor FOXO1 to the CD20 promoter was increased approximately threefold after knockdown of CBP, whereas it was unaffected after knockdown of EP300 (Figure 3C).

Taken together, these results suggest that depletion of CBP or EP300 can affect binding of the CD20 regulators PU.1 and FOXO1 to the CD20 promoter.

Rituximab- and obinutuzumab-induced complement-dependent cytotoxicity in CBP and EP300 knockdown cells

Rituximab is a type I CD20 antibody that has been utilized in the treatment of DLBCL for more than 10 years. Rituximab-mediated cytotoxicity depends on a combination of complement-dependent cytotoxicity (CDC), direct cell death (DCD), and antibody-dependent cellular cytotoxicity (ADCC). The recently introduced glycoengineered type II CD20 antibody obinutuzumab has exhibited increased DCD and ADCC, but decreased CDC. as compared with rituximab [27].

A direct correlation between complement CDC induced by anti-CD20 antibodies and the number of CD20 molecules on the surface of lymphoma cells has been reported [28]. As CBP/EP300 knockdown in SUDHL4 cells reduced CD20 expression (Figure 1), we investigated CDC in response to rituximab or obinutuzumab as described under Methods.

As illustrated in Figure 4, treatment with rituximab or obinutuzumab induced dose-dependent CDC in control cells. Already at a low concentration (1 μg/mL), rituximab strongly induced CDC, as expected from a type I antibody [29]. The cytotoxicity of both antibodies was significantly lower after knockdown of CBP (Figure 4), suggesting that depletion of CBP confers resistance to rituximab- and obinutuzumab-mediated

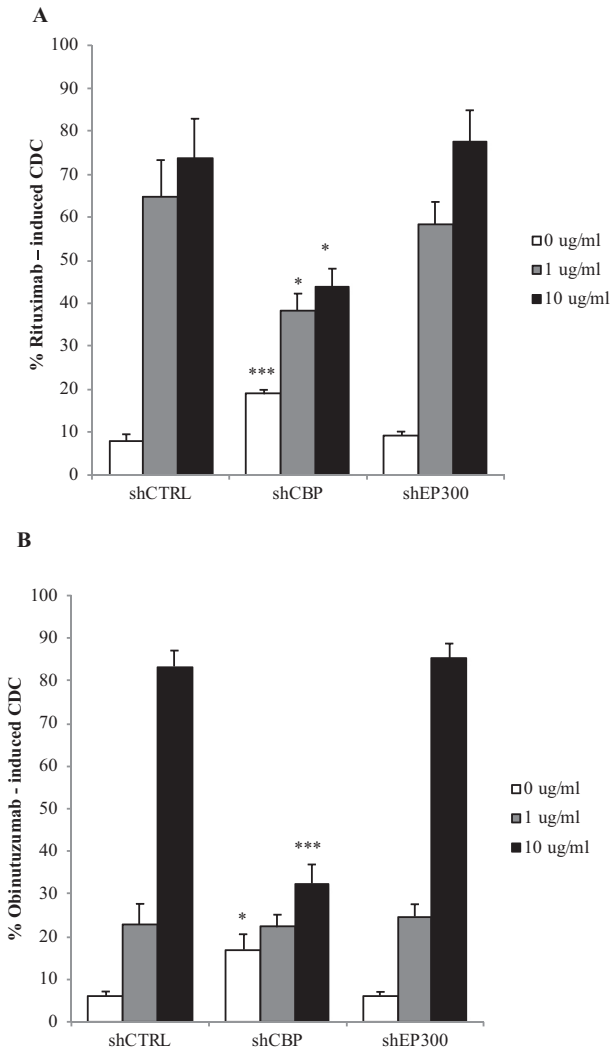

Figure 4. Depletion of CBP impairs rituximab- and obinutuzumab-mediated complement-dependent cytotoxicity in SU-DHL4 cells. Control, CBP, or EP300 knockdown cells were incubated for 2 hours with rituximab **(A)** or obinutuzumab **(B)** in the presence of 10% human serum as complement source. Cell viability was measured with PI staining through flow cytometry (±SEM). The statistical significance of differences between control and transduced cells was determined with two-tailed unpaired Student *t* tests. Asterisks indicate the statistical significance of differences between knockdown cells and control at each antibody concentration (*$p \leq 0.05$, ***$p \leq 0.001$, $n = 4$). Nonsignificant *p* values are not shown in the graph. Two-way analysis of variance test revealed significant interaction within shCTRL, shCBP, and shEP300 transfected cells in response to different concentrations of rituximab or obinutuzumab ($p < 0.01$).

CDC. Knockdown of EP300, on the other hand, had no significant effect on either rituximab- or obinutuzumab-induced CDC. The difference in antibody resistance between CBP and EP300 knockdown cells may be related to the stronger repression of CD20 expression after CBP knockdown (Figure 1).

Rituximab- and obinutuzumab-induced DCD in CBP and EP300 knockdown cells

In addition to CDC, anti-CD20 antibodies can also induce DCD [30]. To evaluate the effect of rituximab- and obinutuzumab-induced DCD after knockdown of CBP or EP300, DCD was analyzed as described under Material and Methods. Both antibodies induced DCD, with expected stronger effects from the type II antibody obinutuzumab [29]. The results indicate that rituximab-induced DCD was significantly reduced in both CBP and EP300 knockdown cells, as compared with the control (Figure 5A). Obinutuzumab induced somewhat higher levels of DCD, as compared to rituximab (Figure 5B), consistent with previous reports [29,31]. Knockdown of CBP conferred increased resistance to obinutuzumab-induced DCD, while a small reduction in DCD after knockdown of EP300 did not reach statistical significance (Figure 5B). In conclusion, downregulation of both CBP and EP300 affected the efficacy of DCD induced by rituximab and obinutuzumab. However, in line with previous reports indicating that obinutuzumab shows enhanced DCD, as compared with rituximab [29,31] obinutuzumab-induced DCD is less affected by loss of CBP or EP300.

Rituximab- and obinutuzumab-induced ADCC in CBP and EP300 knockdown cells

Cytotoxic effects of antibodies include ADCC [30], and obinutuzumab has been reported to exert increased ADCC as compared with rituximab [27,29]. To evaluate whether the suppression of CBP or EP300 could affect ADCC, CBP and EP300 knockdown cells were incubated with anti-CD20 antibodies in the presence of NK cells, as described under Methods. As expected, the type II antibody obinutuzumab, as compared with rituximab, exhibited slightly higher ADCC in control cells. However, no significant differences in ADCC in response to rituximab or obinutuzumab were observed in CBP or EP300 knockdown cells, as compared with control cells (Figure 6). This is consistent with previous reports suggesting that ADCC has a substantially lower threshold for the density of CD20 on the cell surface, as compared with CDC and DCD [32].

Discussion

Antibodies directed against CD20 are a cornerstone in the treatment of DLBCL. However, suboptimal response rates and anti-CD20 resistance at relapse are clinical problems, to some extent dependent on decreased cell surface expression of CD20 [2,3]. Expression of CD20 is epigenetically regulated [33], and epigenetic regulators are recurrently mutated in DLBCL [34]. Among these, the acetyltransferases CBP and EP300 are indicated as tumor suppressors, as suggested by the predominance of monoallelic inactivating

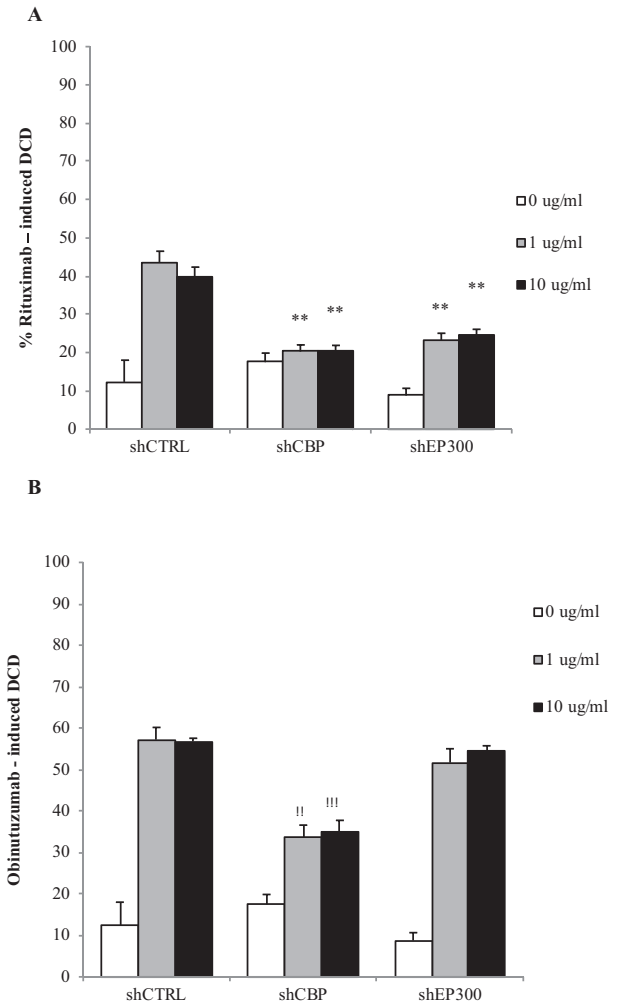

Figure 5. Rituximab- and obinutuzumab-mediated direct cell death is impaired by CBP or EP300 reduction in SU-DHL4 cells. Control, CBP, or EP300 knockdown cells were incubated for 2 hours with rituximab **(A)** or obinutuzumab **(B)**, and the apoptotic-dead cells were assessed by phosphatidylserine exposure and PI staining through flow cytometry analysis. The graphs depict the mean percentage of total Annexin V/PI double-positive cells (±SEM). Statistical significance of differences between control and transduced cells was determined with two-tailed unpaired Student *t* tests. Asterisks indicate the statistical significance of differences between knockdown cells and control at each antibody concentration (**$p \leq 0.01$, ***$p \leq 0.001$, $n = 3$). Nonsignificant *p* values are not shown in the graph. A two-way analysis of variance test revealed significant interaction within shCTRL, shCBP, and shEP300 transfected cells in response to different concentrations of rituximab or obinutuzumab ($p < 0.001$).

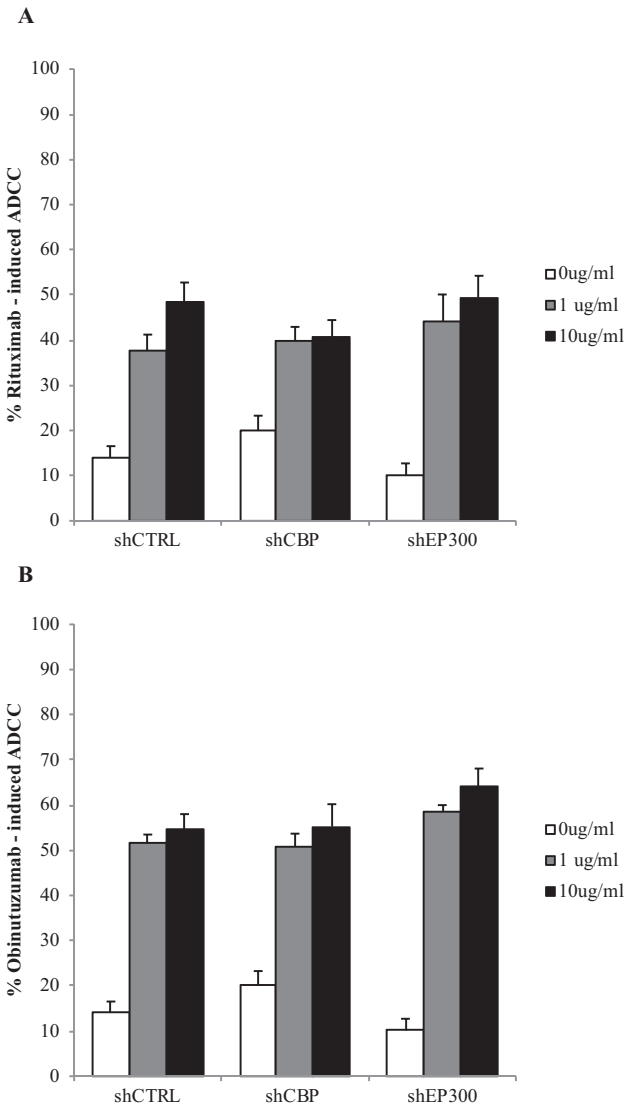

Figure 6. Antibody-dependent cell cytotoxicity induced by rituximab and obinutuzumab in CBP or EP300 knockdown cells. Control, CBP or EP300 knockdown cells were previously stained with DIOC18 and then incubated for 2 hours with rituximab **(A)** or obinutuzumab **(B)** in the presence of natural killer cells. Target cell death was estimated by DIOC18/PI positivity as judged by flow cytometry. Graphs depict the mean percentage of total DIOC18+PI+ cells (±SEM). Statistical significance of differences between control and transduced cells was determined with two-tailed unpaired Student *t* tests, which revealed no statistically significant differences ($n = 3$). Nonsignificant *p* values are not shown in the graph. Two-way analysis of variance test revealed nonsignificant interaction within shCTRL, shCBP, and shEP300 cells in response to different concentrations of rituximab or obinutuzumab ($p > 0.05$).

mutations [9,11]. In this study, we found that reduced levels of CBP or EP300 in the DLBCL cell line (SU-DHL4) downregulate CD20 expression and increase the resistance to anti-CD20 antibodies.

As mutation of CBP and EP300 is more common in GC-derived lymphomas than in lymphomas of the activated B-cell type, the GC-derived DLBCL cell line SU-DHL4 was chosen as the model. SU-DHL4 also has the advantage of carrying wild-type *CBP* and *EP300* genes. Unfortunately, we were not able to identify other DLBCL cell lines carrying *CBP* and *EP300* wild-type genes. Nevertheless, the downregulation of CD20 mRNA in response to depletion of CBP or

EP300 was confirmed in the GC B-cell lymphoma cell line WSU-NHL, carrying an inactivating mutation in the histone acetyl transferase domain of CBP (Supplementary Figure E2).

Our conclusion that adequate levels of CBP and EP300 are important for CD20 expression is based on our observation that shRNA-mediated knockdown of either CBP or EP300 reduces the amount of CD20 at the levels of mRNA and protein, as well as cell surface expression. Our results are consistent with previous reports on the sensitivity of CD20 levels to epigenetic manipulation by HDAC inhibition both in vitro [4,6] and in vivo [7].

Thus, our data strongly support the involvement of CBP and EP300 in transcriptional regulation of CD20. The precise mechanism of action is, however, not clear. Unexpectedly, we could not detect obvious differences in acetylation of H3K9 and H3K27 on the CD20 promoter in CBP or EP300 knockdown cells. However, besides histone acetylation, CBP and EP300 can acetylate specific transcription factors [16]. Our present observations that CBP and EP300 affect the binding of PU.1 and FOXO1 to the CD20 promoter suggest that these transcription factors may be functionally modulated by acetylation by CBP and EP300 also in this context. Given that PU.1 has been reported as a transcriptional activator of CD20 [4,20], our observations that knockdown of either CBP or EP300 resulted in a reduced amount of PU.1 at the CD20 promoter suggests that translational regulation of PU.1 is at least partly involved in the mechanisms by which CBP and EP300 affect CD20 expression (for hypothetical model, see Figure 7). The increased binding of FOXO1 to the CD20 promoter after CBP knockdown is interesting. Activating FOXO1 mutations have been associated with poor response to standard therapy in DLBCL [35], and FOXO1 binding to the CD20 promoter results in transcriptional repression of CD20, with mutant FOXO1 showing even increased repression [23]. Our data thus support the notion of FOXO1 as an important regulator of CD20 and suggest that CBP-mediated acetylation of FOXO1 is involved in the regulation of CD20 in DLBCL. This is consistent with data indicating that CBP-mediated acetylation of FOXO1 decreases DNA binding [25,26]. PU.1 and FOXO1 have overlapping binding sites on the CD20 promoter, and it is possible that depletion of CBP tilts the balance in favor of FOXO1 [6,23].

The type I CD20 antibody rituximab in combination with chemotherapy has been standard treatment in DLBCL for more than a decade. Interindividual responses and development of resistance are, however, remaining clinical problems [36]. One of the potential mechanisms for resistance is decreased expression of CD20 on tumor cells [37–42]. The type II antibody

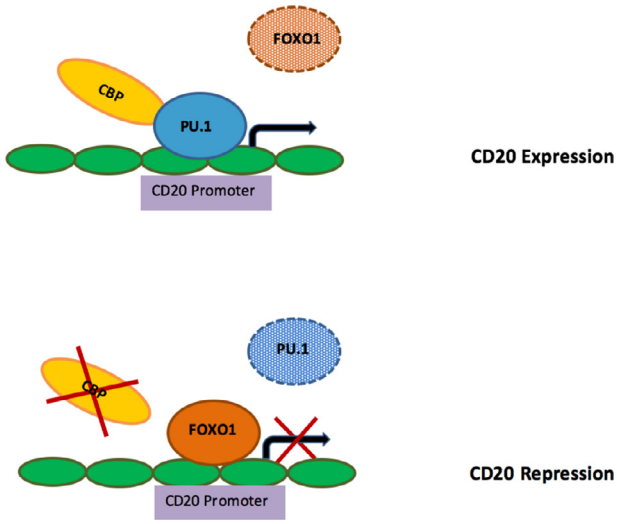

Figure 7. Hypothetical model of regulation of CD20 transcription by PU.1 and FOXO1 in the presence or absence of CBP. In the presence of CBP, PU.1 binds to the CD20 promoter, activating CD20 transcription. PU.1 and FOXO1 have overlapping binding sites, and binding of PU.1 simultaneously displaces FOXO1 (upper panel). Depletion of CBP results in decreased affinity of PU.1 to the CD20 promoter. The reduced binding of PU.1 allows increased binding of FOXO1 to the promoter, resulting in repression of CD20 transcription (lower panel). Please see text for details.

obinutuzumab was developed to overcome mechanisms of resistance, and preclinical studies indicated superior DCD and ADCC, as compared with rituximab [36].

Tsai et al. [2] found that a CD20 antigen surface threshold level is required for effective rituximab-associated CDC. Our observation that knockdown of CBP, and thus CD20, reduces rituximab-induced CDC supports this notion. The effect of rituximab on CDC was, however, not significantly affected after knockdown of EP300, which may be explained by the weaker reduction in CD20 in these cells. On the other hand, at lower concentration (1 μg/mL), obinutuzumab induced less CDC as compared with rituximab, consistent with previous reports indicating that this antibody is a weak inducer of CDC [36]. At a higher concentration, obinutuzumab induced CDC that was significantly reduced after knockdown of CBP, but not of EP300, similar to what was found with rituximab. Interestingly, knockdown of CBP alone resulted in a slight but statistically significant increase in CDC. We cannot explain this phenomenon, but speculate that it is connected to a deranged presentation of complement activating proteins on the cell surface induced by CBP depletion.

Rituximab-induced DCD was reduced after knockdown of CBP, as well as of EP300, emphasizing the importance of CD20 levels. When comparing DCD induced by rituximab and obinutuzumab, the latter, as expected, exhibited showed the strongest effect [29,36]. Both CBP knockdown and EP300 knockdown resulted

in almost abolished rituximab-induced DCD, suggesting a strong dependence on the density of CD20. Interestingly, obinutuzumab-induced DCD was less affected after CBP knockdown and almost unaffected after reduction of EP300. These findings may suggest that obinutuzumab, which acts with a lower threshold of CD20 density on the cell surface for DCD induction, may be a more efficient antibody than rituximab against CBP and EP300 mutant DLBCL cells.

Although obinutuzumab has an advantageous in vitro profile, and is now established as standard treatment in chronic lymphocytic leukemia and follicular lymphoma patients, its potential advantageous effects in the treatment of DLBCL are more unclear. Our findings may suggest that CBP mutant DLBCL patients could profit from intensified treatment with anti-CD20 antibodies, for example, obinutuzumab. Recent results from the phase III GOYA trial including previously untreated DLBCL patients failed to demonstrate a clinical advantage for obinutuzumab, as compared with rituximab, in combination with cyclophosphamide, doxorubicin, oncovin and prednisone (CHOP) [43]. One can only speculate that a hitherto unexplored CBP mutant subgroup in the GOYA trial [44] did benefit from obinutuzumab instead of rituximab. Taken together, our data may suggest that CBP mutant DLBCL patients could benefit from obinutuzumab treatment. Future trials are warranted to explore this notion.

Conclusions

Expression of CD20 is sensitive to epigenetic regulation, and levels of CD20 affect the response to anti-CD20 antibodies. We found that depletion of the commonly mutated histone acetyltransferases CBP and EP300 leads to a pronounced reduction of levels of CD20 mRNA and protein in DLBCL cells. Moreover, the response to treatment with the anti-CD20 antibodies rituximab and obinutuzumab is impaired. Reduction of CBP has a stronger effect than reduction of EP300 in this context. Moreover, as compared with rituximab, obinutuzumab seems to partially overcome the negative impact of CBP or EP300 depletion on anti-CD20 antibody cytotoxicity. Future studies are warranted to further explore these issues.

Conflict of interest disclosure

KD is a shareholder and board member of Respiratorius AB. KD has received honoraria from Roche.

Acknowledgments

We thank the Swedish Cancer Society, the Berta Kamprad Foundation, Blodsjukas förening I Södra sjukvårdsregionen, and Swedish governmental funding for clinical research (ALF) (Grant 10602) for generous grants.

We thank our colleagues from the Department of Hematology and Transfusion Medicine. We thank Aitzkoa Lopez de Lapuente Portilla for excellent technical support of FACS experiments. We thank Fredrik Nilsson for excellent statistical support.

References

1. Advani RH, Chen H, Habermann TM, et al. Comparison of conventional prognostic indices in patients older than 60 years with diffuse large B-cell lymphoma treated with R-CHOP in the US Intergroup Study (ECOG 4494, CALGB 9793): consideration of age greater than 70 years in an elderly prognostic index (E-IPI). Br J Haematol. 2010;151:143–151.
2. Tsai PC, Hernandez-Ilizaliturri FJ, Bangia N, Olejniczak SH, Czuczman MS. Regulation of CD20 in rituximab-resistant cell lines and B-cell non-Hodgkin lymphoma. Clin Cancer Res. 2012;18:1039–1050.
3. Kennedy GA, Tey SK, Cobcroft R, et al. Incidence and nature of CD20-negative relapses following rituximab therapy in aggressive B-cell non-Hodgkin's lymphoma: a retrospective review. Br J Haematol. 2002;119:412–416.
4. Sugimoto T, Tomita A, Hiraga J, et al. Escape mechanisms from antibody therapy to lymphoma cells: downregulation of CD20 mRNA by recruitment of the HDAC complex and not by DNA methylation. Biochem Biophys Res Commun. 2009;390:48–53.
5. Pozzo F, Bittolo T, Arruga F, et al. NOTCH1 mutations associate with low CD20 level in chronic lymphocytic leukemia: evidence for a NOTCH1 mutation-driven epigenetic dysregulation. Leukemia. 2016;30:182–189.
6. Shimizu R, Kikuchi J, Wada T, Ozawa K, Kano Y, Furukawa Y. HDAC inhibitors augment cytotoxic activity of rituximab by upregulating CD20 expression on lymphoma cells. Leukemia. 2010;24:1760–1768.
7. Damm JK, Gordon S, Ehinger M, et al. Pharmacologically relevant doses of valproate upregulate CD20 expression in three diffuse large B-cell lymphoma patients in vivo. Exp Hematol Oncol. 2015;4:4.
8. McCabe MT, Ott HM, Ganji G, et al. EZH2 inhibition as a therapeutic strategy for lymphoma with EZH2-activating mutations. Nature. 2012;492:108–112.
9. Pasqualucci L, Dominguez-Sola D, Chiarenza A, et al. Inactivating mutations of acetyltransferase genes in B-cell lymphoma. Nature. 2011;471:189–195.
10. Ortega-Molina A, Boss IW, Canela A, et al. The histone lysine methyltransferase KMT2D sustains a gene expression program that represses B cell lymphoma development. Nat Med. 2015;21:1199–1208.
11. Jiang Y, Ortega-Molina A, Geng H, et al. CREBBP inactivation promotes the development of HDAC3 dependent lymphomas. Cancer Discov. 2016. CD-16-0975.
12. Santer FR, Hoschele PP, Oh SJ, et al. Inhibition of the acetyltransferases p300 and CBP reveals a targetable function for p300 in the survival and invasion pathways of prostate cancer cell lines. Mol Cancer Ther. 2011;10:1644–1655.
13. Ginzinger DG. Gene quantification using real-time quantitative PCR: an emerging technology hits the mainstream. Exp Hematol. 2002;30:503–512.
14. Zhang J, Vlasevska S, Wells VA, et al. The CREBBP acetyltransferase Is a haploinsufficient tumor suppressor in B-cell lymphoma. Cancer Discov. 2017;7:322–337.
15. Catalogue of somatic mutations in cancer (COSMIC). Sample coss1945197. 2019, September 5. https://cancer.sanger.ac.uk/cosmic.
16. Sterner DE, Berger SL. Acetylation of histones and transcription-related factors. Microbiol Mol Biol Rev. 2000;64:435–459.

17. Gupta P, Gurudutta GU, Saluja D, Tripathi RP. PU.1 and partners: regulation of haematopoietic stem cell fate in normal and malignant haematopoiesis. J Cell Mol Med. 2009;13:4349–4363.
18. Mankai A, Bordron A, Renaudineau Y, et al. Purine-rich box-1-mediated reduced expression of CD20 alters rituximab-induced lysis of chronic lymphocytic leukemia B cells. Cancer Res. 2008;68:7512–7519.
19. Mankai A, Buhe V, Hammadi M, et al. Improvement of rituximab efficiency in chronic lymphocytic leukemia by CpG-mediated upregulation of CD20 expression independently of PU.1. Ann NY Acad Sci. 2009;1173:721–728.
20. Himmelmann A, Riva A, Wilson GL, Lucas BP, Thevenin C, Kehrl JH. PU.1/Pip and basic helix loop helix zipper transcription factors interact with binding sites in the CD20 promoter to help confer lineage- and stage-specific expression of CD20 in B lymphocytes. Blood. 1997;90:3984–3995.
21. Bai Y, Srinivasan L, Perkins L, Atchison ML. Protein acetylation regulates both PU.1 transactivation and Ig kappa 3′ enhancer activity. J Immunol. 2005;175:5160–5169.
22. Ushmorov A, Wirth T. FOXO in B-cell lymphopoiesis and B cell neoplasia. Semin Cancer Biol. 2018;50:132–141.
23. Pyrzynska B, Dwojak M, Zerrouqi A, et al. FOXO1 promotes resistance of non-Hodgkin lymphomas to anti-CD20-based therapy. Oncoimmunology. 2018;7:e1423183.
24. van der Heide LP, Smidt MP. Regulation of FoxO activity by CBP/p300-mediated acetylation. Trends Biochem Sci. 2005;30:81–86.
25. Matsuzaki H, Daitoku H, Hatta M, Aoyama H, Yoshimochi K, Fukamizu A. Acetylation of Foxo1 alters its DNA-binding ability and sensitivity to phosphorylation. Proc Natl Acad Sci USA. 2005;102:11278–11283.
26. Brent MM, Anand R, Marmorstein R. Structural basis for DNA recognition by FoxO1 and its regulation by posttranslational modification. Structure. 2008;16:1407–1416.
27. Tobinai K, Klein C, Oya N, Fingerle-Rowson G. A review of obinutuzumab (GA101), a novel type II anti-CD20 monoclonal antibody, for the treatment of patients with B-cell malignancies. Adv Ther. 2017;34:324–356.
28. Winiarska M, Nowis D, Bil J, et al. Prenyltransferases regulate CD20 protein levels and influence anti-CD20 monoclonal antibody-mediated activation of complement-dependent cytotoxicity. J Biol Chem. 2012;287:31983–31993.
29. Mossner E, Brunker P, Moser S, et al. Increasing the efficacy of CD20 antibody therapy through the engineering of a new type II anti-CD20 antibody with enhanced direct and immune effector cell-mediated B-cell cytotoxicity. Blood. 2010;115:4393–4402.
30. Pescovitz MD. Rituximab, an anti-cd20 monoclonal antibody: history and mechanism of action. Am J Transplant. 2006;6:859–866.
31. Owen C, Stewart DA. Obinutuzumab for the treatment of lymphoproliferative disorders. Expert Opin Biol Ther. 2012;12:343–351.
32. Okroj M, Osterborg A, Blom AM. Effector mechanisms of anti-CD20 monoclonal antibodies in B cell malignancies. Cancer Treat Rev. 2013;39:632–639.
33. Scialdone A, Hasni MS, Damm JK, Lennartsson A, Gullberg U, Drott K. The HDAC inhibitor valproate induces a bivalent status of the CD20 promoter in CLL patients suggesting distinct epigenetic regulation of CD20 expression in CLL in vivo. Oncotarget. 2017;8:37409–37422.
34. Huang YH, Zhao W. Somatic mutations of epigenetic regulator genes in diffuse large B-cell lymphoma. Blood. 2016;128:1756.
35. Morin RD, Assouline S, Alcaide M, et al. Genetic landscapes of relapsed and refractory diffuse large B-cell lymphomas. Clin Cancer Res. 2016;22:2290–2300.
36. Freeman CL, Sehn LH. A tale of two antibodies: obinutuzumab versus rituximab. Br J Haematol. 2018;182:29–45.
37. Hiraga J, Tomita A, Sugimoto T, et al. Down-regulation of CD20 expression in B-cell lymphoma cells after treatment with rituximab-containing combination chemotherapies: its prevalence and clinical significance. Blood. 2009;113:4885–4893.
38. Davis TA, Czerwinski DK, Levy R. Therapy of B-cell lymphoma with anti-CD20 antibodies can result in the loss of CD20 antigen expression. Clin Cancer Res. 1999;5:611–615.
39. van Meerten T, van Rijn RS, Hol S, Hagenbeek A, Ebeling SB. Complement-induced cell death by rituximab depends on CD20 expression level and acts complementary to antibody-dependent cellular cytotoxicity. Clin Cancer Res. 2006;12:4027–4035.
40. Golay J, Lazzari M, Facchinetti V, et al. CD20 levels determine the in vitro susceptibility to rituximab and complement of B-cell chronic lymphocytic leukemia: further regulation by CD55 and CD59. Blood. 2001;98:3383–3389.
41. Wojciechowski W, Li H, Marshall S, Dell'Agnola C, Espinoza-Delgado I. Enhanced expression of CD20 in human tumor B cells is controlled through ERK-dependent mechanisms. J Immunol. 2005;174:7859–7868.
42. Bobrowicz M, Dwojak M, Pyrzynska B, et al. HDAC6 inhibition upregulates CD20 levels and increases the efficacy of anti-CD20 monoclonal antibodies. Blood. 2017;130:1628–1638.
43. Vitolo U, Trneny M, Belada D, et al. Obinutuzumab or rituximab plus cyclophosphamide, doxorubicin, vincristine, and prednisone in previously untreated diffuse large B-cell lymphoma. J Clin Oncol. 2017;35:3529–3537.
44. Vitolo U, Trněný M, Belada D, et al. Obinutuzumab or rituximab plus CHOP in patients with previously untreated diffuse large B-cell lymphoma: Final results from an open-label, randomized phase 3 study (GOYA). Blood. 2016;128:470.

Supplementary Table 1. Primers for amplification of CBP and EP300 genes from exon 24 to exon 31, encoding the acetyl transferase domain of both proteins.

CREBBP PCR primers	EP300 PCR primers
exon 24	**exons 24-25**
F: ctgcaaagtggggtggattc	*F:* gattagcatgttccctgcactc
R: ggatgacctcaaactcaagagc	*R:* ttgcatttccaaaccaaacac
exon 25	
F: cagagttagaggagcaggcc	
R: ggacacttaagagccctggt	
exon 26	**exon 26**
F: ccagggtgttgtttgttgct	*F:* caaagagcctgggagagtgag
R: agggaaagagcttgctacgt	*R:* gggccaacatatccatttctc
exon 27	**exon 27**
F: tggttacttctgtcctggct	*F:* ggtatctatatcaactccaacttgtgg
R: cctcccctcagttgtgacaa	*R:* gaatggcatgaacccagg
exon 28	**exon 28**
F: atggccctcatctcactgtt	*F:* gcttaggtataaagtctctgccagc
R: gtgcatgtgtgaacggagac	*R:* aaagtttaataccactgaaacagaacc
exon29	**exon 29**
F: ggtgacctactttggcctga	*F:* accaaggtcttctggctcc
R: ctgcgagtctttccctcctc	*R:* gcccagcgaacagtcagt
exon 30	**exon 30**
F: gtgccatgtcccttgtgtg	*F:* ccatggtgggataattgcttg
R: caaagggacaggatgcttcg	*R:* aaatacgtggctgcatggc
exon 31(a)	**exon 31(a)**
F: tggcacagacccagacttag	*F:* gggcagagctgaagaggc
R: tgttgttgatgttcacccgg	*R:* cttgagtcctgggcaagtagg
exon 31(b)	**exon 31(b)**
F: cctgtaccgggtgaacatca	*F:* tgcctaaacatcaagcagaagc
R: cggtactgtggattcatcgc	*R:* aggcttgttgagacacagtgc
exon 31(b2)	**exon 31(c)**
F: ccaagtacgtggccaatcag	*F:* aacctttgaacatggctccac
R: tactaagggacgtggcgatc	*R:* catctgttgctgaaggagtcg
exon 31(c)	
F: caacagcagatgaagcagca	
R: aacttctctagcgtgtcccc	

Supplementary Table 2. Primers for sequencing of CBP and EP300 genes: from exon 24 to exon 31.

CREBBP sequencing primers	EP300 sequencing primers
exon 24	**exon 24**
F: ggctgcagaccacaagact	*F: gttgccatctaccagacttgg*
R: gtgacttcatcccgggctt	*R:* cttgctttcatgcctggttt
exon 25	**exon 25**
F: tggggaaatgtctgaatctttcc	*F:* tgtggacagtggagagatgg
R: tcagagccgtattcttggac	*R:* gagggcagtcagagccatac
exon 26	**exon 26**
F: aaacatgtgcctccttccca	*F:* gtgagagggtgttattaggca
R: tctcatggtaaacggctgtg	*R:* actgcagtcctcaagcattt
exon 27	**exon 27**
F: cctgtcctccaagtgaagga	*F:* acacaacagggcatatttgg
R: cgccttgtccagcatctttt	*R:* catggacaatacgctctgataca
exon 28	**exon 28**
F: ctcaccagtgccaaggaac	*F:* agctactgaagatagattaacaagtgc
R: ctgcagtgctctcttccttt	*R:* tctgtgctttcattgctggt
exon29	**exon29**
F: acagccttgcgtgttgttg	*F:* gaccaagggagacagcaaaa
R: tccttgtgcttctccatggt	*R:* gcttctccatggtggcata
exon 30	**exon 30**
F: ttcttcgtgatccacctgca	*F:* tctttgtgatccgcctcatt
R: actcgttgcaggtgtagaca	*R:* cttgcattcattgcaggtgt
exon 31(a)	**exon 31(a)**
F: tggcacagacccagacttag	*F:* ccagaagatgaagcgggttg
R: ggtaggcttccctgtggac	*R:* catttgggcctgctgtagtc
exon 31(b)	**exon 31(b)**
F: cagcctgcagaacctgaatg	*F:* caatccaacaccagatgccc
R: tcctgagagcatgtgttgct	*R:* tcccagactgtagttgctgg
exon 31(c)	**exon 31(c)**
F: gatcgccacgtcccttagta	*F:* gaacatggctccacaaccag
R: tgcatggatatcacaggcct	*R:* tgcttgatgaatgcagccaa
exon 31(d)	**exon 31(d)**
F: gatcgccacgtcccttagta	*F:* cacaacaccatgccttcaca
R: ttccccaagtgtccctgatc	*R:* gctggcctatctgtcccata

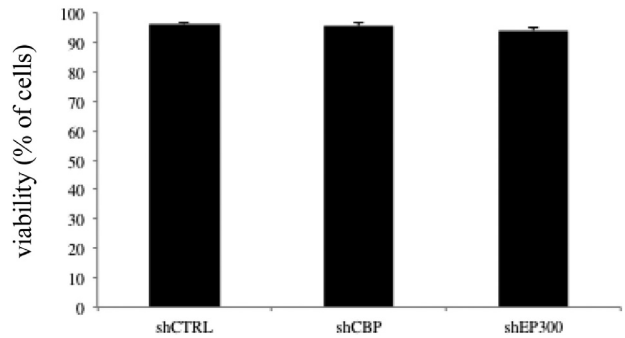

Supplementary Fig. 1. The viability of SU-DHL4 cells transduced with shCTRL, shCBP or shEP300 was determined using trypan blue exclusion (± SEM; *n=8*). Non-significant *p* values are not shown.

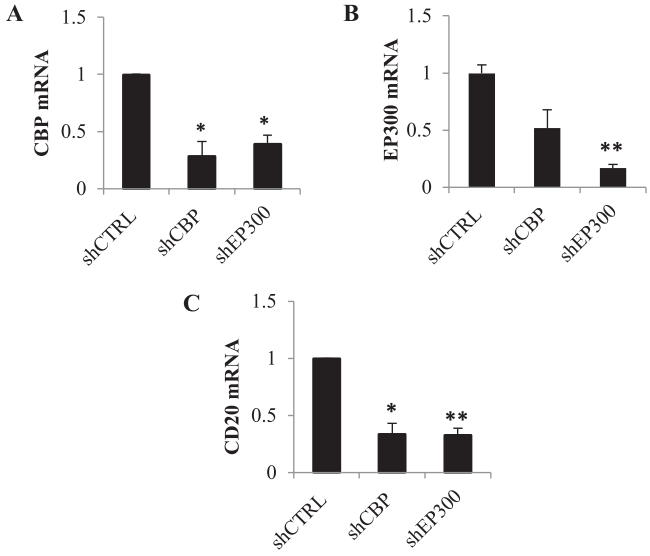

Supplementary Fig. 2. WSU-NHL cells were transduced with shRNA targeting either CBP or EP300. Expression of CBP **(A)**, EP300 **(B)** and CD20 **(C)** mRNA was determined by qPCR (±SEM; *n=3*). Statistical significance was determined with two tailed unpaired Student's t-test. Stars indicate statistical significance (*$p \leq 0{,}05$; **$p \leq 0{,}01$; ***$p \leq 0{,}001$). Non-significant *p* values are not shown in the graph.